

## Article

# Proportional-Switch Adjustment Process-Based Day-by-Day Evolution Model for Mixed Traffic Flow in an Autonomous Driving Environment

Yihao Huang<sup>1,2</sup>, Han Zhang<sup>3</sup> and Aiwu Kuang<sup>4,\*</sup>

<sup>1</sup> Department of Automotive Engineering, Xiangtan Technician College, Xiangtan 411100, China; huangyihao9235@gmail.com

<sup>2</sup> Department of Automotive Engineering, Xiangtan Vocational College of Science and Technology, Xiangtan 411100, China

<sup>3</sup> Henan Vocational College of Water Conservancy and Environment, Zhengzhou 450008, China; zhanghan58421@gmail.com

<sup>4</sup> School of Traffic & Transportation Engineering, Changsha University of Science & Technology, Changsha 410114, China

\* Correspondence: jxgakaw@csust.edu.cn; Tel.: +86-139-0748-6326

**Abstract:** Given the rapid development of technologies such as new energy vehicles, autonomous driving, and vehicle-to-everything (V2X) communication, a mixed traffic flow comprising connected and autonomous vehicles (CAVs) and human-driven vehicles (HDVs) is anticipated to emerge. This necessitates the development of a daily dynamic evolution model for mixed traffic flow to address the dynamic traffic management needs of urban environments characterized by mixed traffic. The daily dynamic evolution model can capture the temporal evolution of traffic flow in road networks, with a focus on the daily path choice behavior of travelers and the evolving traffic flow in the network. First, based on the travel characteristics of CAVs and HDVs, the user group in a connected autonomous driving environment is classified into three categories, each adhering to the system optimal (SO) criterion, the user equilibrium (UE) criterion, or the stochastic user equilibrium (SUE) criterion. Next, the pure HDV traffic capacity BPR (Bureau of Public Roads) function is adapted into a heterogeneous traffic flow travel time function to compute the travel time cost for mixed traffic flow. Based on the energy consumption calculation formula for HDVs, the impact of CAVs is fully considered to establish the travel energy consumption cost for both CAVs and HDVs. The total individual travel cost for CAVs and HDVs encompasses both travel time cost and energy consumption cost. Furthermore, a daily dynamic evolution model for mixed traffic flow in a connected autonomous driving environment is developed using the proportional-switch adjustment process (PAP) model. The fundamental properties of the model are validated. Finally, numerical simulations on an N-dimensional (N-D) network confirm the validity and effectiveness of the daily evolution model for mixed traffic flow. A sensitivity analysis of traveler responses in the daily evolution model reveals that, as the sensitivity of CAVs to impedance changes increases, the fluctuations in mixed traffic flow during the early stages of evolution become more pronounced, and the time required to reach a mixed-equilibrium state decreases. Therefore, the PAP-based daily dynamic evolution model for mixed traffic flow effectively captures the evolution process of CAV and HDV mixed traffic flow and supports urban traffic management in a connected autonomous driving environment.

**Keywords:** day-by-day evolution model; mixed traffic flow; N-D network



Academic Editors: Stergios Mavromatis, Yasser Hassan and George Yannis

Received: 14 December 2024

Revised: 10 January 2025

Accepted: 16 January 2025

Published: 20 January 2025

**Citation:** Huang, Y.; Zhang, H.; Kuang, A. Proportional-Switch Adjustment Process-Based Day-by-Day Evolution Model for Mixed Traffic Flow in an Autonomous Driving Environment. *World Electr. Veh. J.* **2025**, *16*, 53. <https://doi.org/10.3390/wevj16010053>

**Copyright:** © 2025 by the authors. Published by MDPI on behalf of the World Electric Vehicle Association. Licensee MDPI, Basel, Switzerland. This article is an open access article distributed under the terms and conditions of the Creative Commons Attribution (CC BY) license (<https://creativecommons.org/licenses/by/4.0/>).

## 1. Introduction

In recent years, with the rapid advancement of technologies such as new energy vehicles, autonomous driving, and vehicle networking, connected and autonomous vehicles (CAVs) have emerged as a novel mode of transportation. CAVs represent a new generation of vehicles capable of autonomous driving and intelligent information exchange between vehicles, roads, people, and the cloud, facilitated by advanced onboard equipment and the integration of modern communication and network technologies. Compared to human-driven vehicles (HDVs), CAVs minimize human involvement in the driving process, reduce vehicle reaction time through onboard sensors, maintain shorter following distances, and enable platoon driving. The introduction of CAVs is expected to increase road capacity and alleviate traffic congestion and pollution. According to the “New Energy Vehicle Industry Development Plan (2021–2035)”, by 2025, China aims to achieve a target where 30% of new car sales consist of intelligent connected vehicles, and, by 2050, the penetration rate of CAVs on the road is projected to reach 75% [1]. It is foreseeable that, in the future, a mixed scenario involving CAVs and HDVs will emerge on the roads. Therefore, the coexistence of autonomous and human-driven vehicles will increase the complexity of traffic flow research, necessitating the optimization of studies on mixed-equilibrium flow.

Due to the advantages of intelligence and automation, the path selection criteria for CAVs differ from those of HDVs, resulting in a mixed traffic equilibrium. Levin et al. modified the traditional four-stage model to analyze the impact of CAV penetration on travel, mode, and route choice. They assumed that both CAVs and HDVs have access to complete network information and adhere to Wardrop’s first principle in route choice. A mixed traffic equilibrium distribution model was then developed based on variational inequalities [2]. Chen et al. examined the planning problem of CAV-dedicated lanes and developed a mixed traffic equilibrium distribution model using nonlinear programming [3]. Li et al. assumed that the path choice of CAV users is fully controllable and proposed a mixed traffic equilibrium distribution model based on the “Stochastic User Equilibrium—System Optimum” framework [4]. Zhang et al. assumed that the path choice of HDV users aims to minimize actual travel impedance, while CAV users aim to reduce the total system cost. They developed a “UE (User Equilibrium)—SO (System Optimum)” traffic equilibrium distribution model based on variational inequality theory [5]. Wang et al. enhanced the road section capacity by modeling it as a function of CAV penetration rate in the study of mixed traffic distribution for CAVs and HDVs. They employed the nested logit model to account for the perceived uncertainty and path overlap for HDVs and applied the UE path selection criterion for CAVs, considering their accurate knowledge of road conditions. Based on this, they proposed a mixed traffic equilibrium distribution model [6].

In real-world road networks, traffic volume evolves due to both external and internal factors. As a result, static traffic distribution models are insufficient for capturing the dynamic evolution of traffic flow and cannot predict the equilibrium state the network will ultimately reach. Traffic flow within a network typically takes several days to reach equilibrium, requiring traffic managers to analyze its dynamic evolution in order to formulate effective traffic control measures. Among these, the daily dynamic traffic evolution model is the most effective approach for studying the transition of road network traffic flow from a non-equilibrium state to equilibrium. Existing daily traffic flow dynamic evolution models primarily focus on a single vehicle type, with limited research addressing the daily dynamic evolution of mixed traffic flow. Cantarella et al. developed a daily dynamic evolution model for a mix of cars and buses, incorporating the adjustment of bus routes based on traffic demand and departure frequency [7]. Li and Yang developed a daily dynamic evolution model for mixed car and bus traffic, considering the acceptance capacity of travelers [8]. Liu et al. developed a daily dynamic evolution model, incorporating travelers’

departure times, traffic information, and passenger psychology [9]. Liang Ying developed a daily dynamic evolution model by considering the influencing factors of car and bus travel and also proposed a corresponding congestion charge model [10]. Kou Zhao developed a dual-mode daily dynamic evolution model by accounting for the differences between cars and buses [11]. Yi Yunfan developed a daily dynamic evolution model for mixed CAV and HDV traffic, considering market penetration rates and travel costs for CAVs [12]. Xu Kai developed a daily dynamic evolution model for mixed autonomous vehicles and conventional travelers, considering the impact of the proportion of autonomous vehicles on network traffic [13].

## 2. Travel Cost of Mixed Traffic Flow

Mixed traffic flow refers to the simultaneous presence of connected and autonomous vehicles (CAVs) and human-driven vehicles (HDVs) on a road network. The difference in control mechanisms between CAVs and HDVs leads to a significant disparity in the amount of information accessible to each vehicle type. Although CAVs acquire more information and offer recommendations, there are instances in which travelers may not comply. Accordingly, travelers can be classified into three categories: the first category consists of travelers who fully comply with CAVs, following the system optimum (SO) criterion; the second category includes travelers who do not fully comply with CAVs, adhering to the user equilibrium (UE) criterion; and the third category comprises drivers of HDVs, following the stochastic user equilibrium (SUE) criterion. Ultimately, the equilibrium state of the road network will manifest in three forms: system optimum (SO), user equilibrium (UE), and stochastic user equilibrium (SUE). Research suggests that there are distinct differences in the travel costs associated with CAVs and HDVs. Therefore, separate methods for calculating the travel costs of CAVs and HDVs are developed, encompassing both travel time costs and energy consumption costs.

### 2.1. Travel Time Cost

Based on the heterogeneous traffic flow characteristics of CAVs and HDVs, this paper employs the Bureau of Public Roads (BPR) function, which directly adjusts traffic capacity as the travel time function for heterogeneous traffic flow. Research has shown that, in practice, CAVs maintain a smaller following distance, thereby increasing the road capacity. Therefore, this paper assumes that the road capacity in sections with CAVs will be greater than in sections with only HDVs. Accordingly, this paper introduces a road capacity correction coefficient to adjust the road capacity in a pure HDV environment, where  $\psi_a \geq 1$ .

Research has shown that, on the same road section, the free-flow time for CAVs is shorter than that for HDVs. Therefore, this paper introduces a free-flow time correction coefficient  $\xi_a$  to adjust the free-flow time for HDVs, where  $\xi_a \leq 1$ .

When only HDVs are present on the road section, the road travel time function can be represented as the following BPR function model:

$$t_{a,H}(d) = t_{a,H}^0 \left[ 1 + \alpha \left( \frac{q_{a,H}(d)}{S_{a,H}} \right)^\beta \right] \quad (1)$$

In the formula,  $t_{a,H}(d)$  represents the travel time of HDVs on the road section  $a$  on day  $d$ ,  $t_{a,H}^0$  represents the free-flow time of HDVs on the road section  $a$ ,  $q_{a,H}(d)$  represents the traffic volume of HDVs on the road section  $a$  on day  $d$ , and  $S_{a,H}$  represents the traffic capacity of the road section with only HDVs.

On mixed traffic sections with CAVs and HDVs, the road travel time functions for CAVs and HDVs can be represented, respectively, as follows:

$$t_{a,H}(d) = t_{a,H}^0 \left[ 1 + \alpha \left( \frac{q_{a,H}(d) + q_{a,C}(d)}{\psi_a S_{a,H}} \right)^\beta \right] \quad (2)$$

$$t_{a,C}(d) = \zeta_a t_{a,H}^0 \left[ 1 + \alpha \left( \frac{q_{a,H}(d) + q_{a,C}(d)}{\psi_a S_{a,H}} \right)^\beta \right] \quad (3)$$

In the formula,  $t_{a,C}(d)$  represents the travel time of CAVs on the road section  $a$  on day  $d$ ,  $t_{a,C}^0$  represents the free-flow time of CAVs on the road section  $a$ , and  $q_{a,C}(d)$  represents the traffic volume of CAVs on the road section  $a$  on day  $d$ . Since the addition of CAVs can increase the road capacity, the road capacity correction coefficient  $\psi_a$  is introduced to directly correct the road capacity of the pure HDV section to represent this characteristic.

In summary, the travel time function of heterogeneous traffic flow of CAVs and HDVs can be represented as follows:

$$\begin{cases} t_{a,m}(d) = \zeta_a t_{a,H}^0 \left[ 1 + \alpha \left( \frac{\sum q_{a,m}(d)}{\psi_a S_{a,H}} \right)^\beta \right] \\ \forall m \in M, \forall a \in A, d \geq 0 \end{cases} \quad (4)$$

In the formula,  $t_{a,m}(d)$  represents the travel time of type  $m$  vehicles on road section  $a$  on day  $d$ ,  $t_{a,H}^0$  represents the free-flow time of HDVs on the road section  $a$ ,  $q_{a,m}(d)$  represents the traffic volume of type  $m$  vehicles on road section  $a$  on day  $d$ , and  $S_{a,H}$  represents the traffic capacity of the pure HDV section. When only HDVs are present on the road section,  $\psi_a = 1$  and  $\zeta_a = 1$ .

Next, we can study the function form of the road capacity correction coefficient  $\psi_a$ . Calvert [14] simulated the impact of CAV market penetration on traffic capacity. The research results show that the traffic capacity of pure CAV sections is 68% of the traffic capacity of pure HDVs. Using a univariate quadratic function to fit Calvert's research results, the function form of the road capacity correction coefficient  $\psi_a$  is as follows:

$$\psi_a = b_1 \eta_a^2 + b_2 \eta_a + b_3 = 0.5239 \eta_a^2 + 0.1443 \eta_a + 1.0057, \forall a \in A \quad (5)$$

In the formula,  $\eta_a$  represents the penetration rate of CAV on the road section  $a$ ,  $\eta_a = \frac{q_{a,C}(d)}{q_{a,H}(d) + q_{a,C}(d)}$ ;  $b_1$ ,  $b_2$ , and  $b_3$  are the parameters of the univariate quadratic function.

According to the impedance function, the travel time costs of CAVs and HDVs can be obtained as follows:

$$T_{a,m}(d) = \sum_d \sum_a \sum_m VOT_m \cdot t_{a,m}(d) \cdot q_{a,m}(d), \forall m \in M, \forall a \in A, d \geq 0 \quad (6)$$

In the formula,  $T_{a,m}(d)$  represents the travel time cost of type  $m$  vehicles on road section  $a$  on day  $d$ ,  $VOT_m$  represents the value of time per unit for type  $m$  vehicles,  $t_{a,m}(d)$  represents the impedance function of type  $m$  vehicles on road section  $a$  on day  $d$ , and  $q_{a,m}(d)$  represents the traffic volume of type  $m$  vehicles on road section  $a$  on day  $d$ .

## 2.2. Travel Energy Consumption Cost

This paper draws on the findings of Wadud [15], which indicate that the impact of CAVs on energy consumption ranges from 5% to 20%. Building on the energy consumption calculation formula for HDVs, as proposed by Zhang et al. [16], this paper defines the travel energy consumption cost function for a mixed traffic of CAVs and HDVs as follows:

$$E_{a,m}(d) = \chi\mu\phi\left(\frac{l_a}{t_{a,m}(d)}\right)^{-\gamma} l_a \quad (7)$$

In the formula,  $E_{a,m}(d)$  is the cost of energy consumption per kilometer for type  $m$  vehicles on road section  $a$  on day  $d$ ,  $t_{a,m}(d)$  is the travel time for type  $m$  vehicles on road section  $a$  on day  $d$ ,  $l_a$  is the distance of road section  $a$ ,  $\phi$  and  $\gamma$  are related coefficients, according to the calibration of Zhang [16], whereby  $\phi$  is taken as 147.92 and  $\gamma$  is 0.689,  $\chi$  is 7.8, and  $\mu$  is the degree of CAVs' impact on energy when calculating the travel energy consumption of CAVs.  $\mu$  can be taken as 90% when calculating the energy consumption of HDVs, and, in this case,  $\mu$  is taken as 1.

### 2.3. Total Travel Cost

In summary, the total personal travel cost for CAVs and HDVs encompasses travel time costs, fixed costs, and energy consumption costs, as represented by the following formula:

$$C_{a,m}(d) = T_{a,m}(d) + E_{a,m}(d) \quad (8)$$

In the formula,  $C_{a,m}(d)$  represents the total personal travel cost of type  $m$  vehicles on road section  $a$  on day  $d$ ,  $T_{a,m}(d)$  represents the travel time cost of type  $m$  vehicles on road section  $a$  on day  $d$ , and  $E_{a,m}(d)$  is the cost of energy consumption per kilometer for type  $m$  vehicles on road section  $a$  on day  $d$ .

The total travel cost of CAVs and HDVs on the path is as follows:

$$C_{k,m}^w(d) = \sum_a C_{a,m}(d) \cdot \delta_{a,k}^w \quad (9)$$

In the formula,  $C_{k,m}^w(d)$  represents the total travel cost of type  $m$  vehicles on path  $k$  between the OD pair  $w$  on day  $d$ ;  $\delta_{a,k}^w$  is the section–path-related variable, that is, a 0–1 variable. If section  $a$  belongs to the  $k$  path between the OD pair  $w$ , then  $\delta_{a,k}^w = 1$ ; otherwise,  $\delta_{a,k}^w = 0$ .

## 3. Daily Dynamic Evolution Model for Mixed Traffic Flow

### 3.1. Development of a Day-by-Day Evolution Model for Mixed Traffic Flow

This paper presents a day-by-day dynamic evolution model of mixed traffic flow consisting of CAVs and HDVs, based on the proportional adjustment model.

The path selection adjustment process of type  $m$  vehicles on path  $k$  between the OD pair  $w$  on two consecutive days is as follows:

$$f_{k,m}^w(d+1) - f_{k,m}^w(d) = \sum_{l \in K} f_{l,m}^w(d) \rho_{lk,m}^w(d) - f_{k,m}^w(d) \sum_{l \in K} \rho_{kl,m}^w(d) \quad (10)$$

$$\forall k \in K, \forall w \in W, d \geq 0$$

In the formula,  $f_{k,m}^w(d)$  represents the traffic volume of type  $m$  vehicles on path  $k$  between the OD pair  $w$  on day  $d$ , where the difference in traffic volume of type  $m$  vehicles on the same path on two consecutive days is equal to the input traffic volume on that path minus the output traffic volume.

$\rho_{kl,m}^w(d)$  represents the proportion of type  $m$  vehicles transferred from path  $k$  to path  $l$  between the OD pair  $w$  on day  $d$ , that is, the traffic volume adjustment ratio. At the same time, to avoid excessive adjustment, the traffic volume adjustment ratio needs to be between 0 and 1.

Assuming that  $\rho_{kl,m}^w(d)$  is a function of the difference in generalized travel costs between the two paths, the traffic volume adjustment ratio formula is obtained as follows:

$$\rho_{kl,m}^w(d) = \max \left\{ 0, \frac{1}{|R_k^w(d)| + \zeta} \left[ 1 - \exp \left( -\theta_m^w \frac{C_{k,m}^w(d) - C_{l,m}^w(d)}{C_{k,m}^w(d)} \right) \right] \right\} \quad (11)$$

$$\forall k \in K, \forall l \in K, \forall w \in W, d \geq 0$$

The formula represents the number of target adjustment path set elements on path  $k$  between the origin–destination (OD) pair  $w$  on day  $d$ . To avoid  $|R_k^w(d)| = 0$ , an infinitesimal positive number  $\zeta$  is added to ensure that the denominator is not equal to 0;  $C_{k,m}^w(d)$  represents the generalized travel cost of type  $m$  vehicles on path  $k$  between the OD pair  $w$  on day  $d$ ;  $\theta_m^w$  is the sensitivity of vehicles, representing the sensitivity of type  $m$  vehicles to impedance changes in the origin–destination (OD) pair  $w$ .

Simultaneously, to prevent non-negative adjustments, it is assumed that travelers shift from paths with a high generalized travel cost to paths with a low generalized travel cost. The formula for the target adjustment path  $k$  set between the origin–destination (OD) pair  $w$  on day  $d$  is derived as follows:

$$R_k^w(d) = \{ l \in K : C_{k,m}^w(d) - C_{l,m}^w(d) > 0 \}, \forall k \in K, d \geq 0 \quad (12)$$

The generalized travel cost for different types of travelers is defined as the sum of the time value cost and the travel energy consumption cost. Given that CAVs possess a certain degree of autonomous driving capability, the time values for HDVs and CAVs differ. Therefore, the generalized travel cost formula for type  $m$  vehicles on path  $k$  between the origin–destination (OD) pair  $w$  on day  $d$  is expressed as follows:

$$C_{k,m}^w(d) = \sum_a C_{a,m}(d) \cdot \delta_{a,k}^w, \forall k \in K, d \geq 0 \quad (13)$$

The generalized travel cost for the road section is expressed as follows:

$$C_{a,m}(d) = T_{a,m}(d) + E_{a,m}(d) \quad (14)$$

In the formula,  $C_{a,m}(d)$  represents the total personal travel cost of type  $m$  vehicles on road section  $a$  on day  $d$ ,  $T_{a,m}(d)$  represents the travel time cost of type  $m$  vehicles on road section  $a$  on day  $d$ , and  $E_{a,m}(d)$  is the energy consumption cost per kilometer for type  $m$  vehicles on road section  $a$  on day  $d$ .

The section flow for different types of travelers is equal to the sum of the flow across all paths through the section, meaning that path flow is additive. Therefore, the traffic volume for type  $m$  vehicles on section  $a$  on day  $d$  is expressed as follows:

$$q_{a,m}(d) = \sum_a \delta_{a,k}^w f_{k,m}^w(d), \forall k \in K, d \geq 0 \quad (15)$$

The origin–destination (OD) traffic demand for different types of travelers is equal to the sum of the traffic volume for type  $m$  vehicles on all paths between the OD pair  $w$  on day  $d$ , and the path flow is non-negative. Therefore, the traffic demand for type  $m$  vehicles between the OD pair  $w$  is expressed as follows:

$$Q_m^w = \sum_k \phi_k^w f_{k,m}^w(d), \forall k \in K, \forall w \in W, d \geq 0, f_{k,m}^w(d) \geq 0 \quad (16)$$

In the formula,  $\phi_k^w$  is the path–OD pair-related variable, a 0–1 variable. If path  $k$  connects the OD pair  $w$ , then  $\phi_k^w = 1$ ; otherwise,  $\phi_k^w = 0$ .

### 3.2. Model Theoretical Analysis

In this section, we introduce the fundamental properties of the daily dynamic evolution model within the connected autonomous driving environment and provide a formal proof.

**Proposition 1.** (No Excessive Adjustment): *The traffic volume adjusted out of a path at any single time step will not exceed the initial traffic volume of that path. This relationship is expressed mathematically as follows:*

$$0 \leq \sum_l \rho_{kl,m}^w(d) \leq 1, \forall k \in K, \forall l \in K, \forall w \in W, d \geq 0 \tag{17}$$

**Proof of Proposition 1.** Because

$$1 - \exp\left(-\theta_m^w \frac{C_{k,m}^w(d) - C_{l,m}^w(d)}{C_{k,m}^w(d)}\right) \leq 1 \tag{18}$$

we obtain

$$0 \leq \max\left\{0, 1 - \exp\left(-\theta_m^w \frac{C_{k,m}^w(d) - C_{l,m}^w(d)}{C_{k,m}^w(d)}\right)\right\} \leq 1 \forall k \in K, \forall l \in K, \forall w \in W, d \geq 0 \tag{19}$$

hence, we have

$$\begin{aligned} \sum_l \rho_{kl,m}^w(d) &= \sum_l \max\left\{0, \frac{1}{|R_k^w(d)| + \zeta} \left[1 - \exp\left(-\theta_m^w \frac{C_{k,m}^w(d) - C_{l,m}^w(d)}{C_{k,m}^w(d)}\right)\right]\right\} \\ &\leq \frac{1}{|R_k^w(d)|} |R_k^w(d)| = 1 \end{aligned} \tag{20}$$

Then, the traffic volume adjustment ratio is  $\rho_{kl,m}^w(d) \in [0, 1]$ , and there is no excessive adjustment problem in the path selection adjustment process model.  $\square$

**Proposition 2.** (Solution Set Invariance): *If the initial path selection and traffic volume allocation scheme is feasible, then the path selection and traffic volume allocation scheme generated through iterations of the path selection adjustment process model will also remain feasible. This property can be expressed mathematically as follows:*

$$Q_m^w = \sum_k \phi_k^w f_{k,m}^w(d), \forall k \in K, \forall w \in W, d \geq 0, f_{k,m}^w(d) \geq 0 \tag{21}$$

**Proof of Proposition 2.** Proof can be established based on two aspects: traffic volume conservation and the non-negativity of the traffic volume.

Proof of traffic volume conservation:

Because

$$\sum_k \sum_l f_{l,m}^w(d) \rho_{lk,m}^w(d) = \sum_k \sum_l f_{k,m}^w(d) \rho_{kl,m}^w(d) \tag{22}$$

we obtain

$$\begin{aligned} &\sum_{k \in K} f_{k,m}^w(d+1) \\ &= \sum_{k \in K} f_{k,m}^w(d) + \sum_{k \in K} \left( \sum_{l \in K} f_{l,m}^w(d) \rho_{lk,m}^w(d) - f_{k,m}^w(d) \sum_{l \in K} \rho_{kl,m}^w(d) \right) \\ &= \sum_{k \in K} f_{k,m}^w(d) + \sum_k \sum_l f_{l,m}^w(d) \rho_{lk,m}^w(d) - \sum_k \sum_l f_{k,m}^w(d) \rho_{kl,m}^w(d) \\ &= \sum_{k \in K} f_{k,m}^w(d) + 0 = \dots = Q_m^w \end{aligned} \tag{23}$$

Proof of non-negativity of traffic volume:

Because

$$0 \leq \sum_l \rho_{kl,m}^w(d) \leq 1, \forall k \in K, \forall l \in K, \forall w \in W, d \geq 0 \tag{24}$$

from Equation (1), we obtain

$$\begin{aligned} f_{k,m}^w(d+1) &= f_{k,m}^w(d) + \sum_{l \in K} f_{l,m}^w(d) \rho_{lk,m}^w(d) - f_{k,m}^w(d) \sum_{l \in K} \rho_{kl,m}^w(d) \\ &\geq f_{k,m}^w(d) + \sum_{l \in K} f_{l,m}^w(d) \rho_{lk,m}^w(d) - f_{k,m}^w(d) \\ &= \sum_{l \in K} f_{l,m}^w(d) \rho_{lk,m}^w(d) \geq 0 \end{aligned} \tag{25}$$

By this recursive process, we can obtain the following:

$$f_{k,m}^w(0) \geq 0, \forall k \in K, \forall l \in K, \forall w \in W \tag{26}$$

Then, we obtain the following:

$$f_{k,m}^w(d) \geq 0, \forall k \in K, \forall l \in K, \forall w \in W, d \geq 0 \tag{27}$$

In summary, the path selection adjustment process model demonstrates solution set invariance. □

**Proposition 3.** (Rational Behavior Adjustment Process): Under the condition of a fixed traffic demand, each adjustment process reduces the expected total impedance of the traffic network. When the traffic flow state on the network stabilizes, the network reaches equilibrium. The mathematical expression is as follows:

$$\sum_d \sum_w \sum_k C_{k,m}^w(d) (f_{k,m}^w(d+1) - f_{k,m}^w(d)) \leq 0, \forall k \in K, \forall w \in W, d \geq 0 \tag{28}$$

**Proof of Proposition 3.**

$$\begin{aligned} &\sum_d \sum_w \sum_k C_{k,m}^w(d) (f_{k,m}^w(d+1) - f_{k,m}^w(d)) \\ &= \sum_d \sum_w \sum_k C_{k,m}^w(d) \left( \sum_{l \in K} f_{l,m}^w(d) \rho_{lk,m}^w(d) - f_{k,m}^w(d) \sum_{l \in K} \rho_{kl,m}^w(d) \right) \\ &= \sum_d \sum_w \sum_k \sum_{l \in K} C_{k,m}^w(d) f_{l,m}^w(d) \rho_{lk,m}^w(d) - \sum_d \sum_w \sum_{l \in K} \sum_k C_{l,m}^w(d) f_{l,m}^w(d) \rho_{lk,m}^w(d) \\ &= \sum_d \sum_w \sum_k \sum_{l \in K} C_{k,m}^w(d) f_{l,m}^w(d) \rho_{lk,m}^w(d) - \sum_d \sum_w \sum_k \sum_{l \in K} C_{l,m}^w(d) f_{l,m}^w(d) \rho_{lk,m}^w(d) \\ &= \sum_d \sum_w \sum_k \sum_{l \in K} (C_{k,m}^w(d) - C_{l,m}^w(d)) f_{l,m}^w(d) \rho_{lk,m}^w(d) \end{aligned} \tag{29}$$

From Proposition 1, we obtain  $\sum_d \sum_w \sum_k C_{k,m}^w(d) (f_{k,m}^w(d+1) - f_{k,m}^w(d)) \leq 0$ . □

**Proposition 4.** (Mixed User Equilibrium): Assuming that the traffic demand is fixed, when the network is in a state of mixed user equilibrium, for any type  $m$  traveler between any OD pair  $w$ , all utilized paths between this OD pair have equal and minimum travel costs, and all unused path impedances are greater than this minimum travel cost—that is, no type of traveler can reduce their travel costs by changing their travel plan. The mathematical expression is as follows:

$$\begin{cases} C_{k,m}^w(d) = u_m^w(d), \text{ if } f_{k,m}^w(d) > 0 \\ C_{k,m}^w(d) \geq u_m^w(d), \text{ if } f_{k,m}^w(d) = 0 \end{cases} \forall k \in K, w \in W \tag{30}$$

where  $u_m^w(d)$  represents the minimum generalized travel cost of the  $m$ -th type of traveler between the OD pair  $w$  on day  $d$ .

**Proposition 5.** (Steady-State Path Flow Pattern): The steady-state path flow pattern is a set composed of a series of network path flow states. If any element is extracted as the initial state, the path selection adjustment process model will not adjust the flow. From Proposition 5, it can be obtained that, when  $f_{k,m}^w(d+1) = f_{k,m}^w(d)$ , the path flow pattern  $f^*$  belongs to the steady-state path flow pattern.

**Proposition 6.** The steady-state path flow pattern of the path selection adjustment process model is equivalent to the mixed user equilibrium state.

**Proof of Proposition 5.** We hereby prove that  $f^* \left( f_{k,m}^w(d+1) = f_{k,m}^w(d), \forall k \in K, \forall w \in W, d \geq 0 \right)$  is equivalent to the mixed user equilibrium state.

Sufficiency:

Assume  $C_{k,m}^w(d) \leq C_{l,m}^w(d), \forall k \in K, \forall l \in K, \forall w \in W, d \geq 0$ , and  $f_{k,m}^w(d) \geq 0$ .

Then, we have  $\rho_{kl,m}^w(d) = 0$ ; further, from Formula (30), we can obtain the following:

If  $f_{k,m}^w(d+1) = f_{k,m}^w(d)$ , then  $\sum f_{l,m}^w(d) \rho_{lk,m}^w(d) = 0$ ; thus,  $\rho_{lk,m}^w(d) \geq 0$  and  $f_{k,m}^w(d) \geq 0$  always hold. Hence, we obtain  $f_{l,m}^w(d) \rho_{lk,m}^w(d) = 0$ . Since  $f_{l,m}^w(d) \rho_{lk,m}^w(d) = 0$ , then  $C_{k,m}^w(d) \leq C_{l,m}^w(d)$ ,  $f_{l,m}^w(d) > 0$ , and, when  $f_{l,m}^w(d) > 0$ ,  $C_{k,m}^w(d) = C_{l,m}^w(d)$  holds. If we set  $C_{k,m}^w(d) = u_m^w(d)$ , we can then obtain that, if  $f_{l,m}^w(d) > 0$ , then  $C_{k,m}^w(d) = u_m^w(d)$ . If  $f_{l,m}^w(d) = 0$ , then  $C_{l,m}^w(d) \geq u_m^w(d)$ , thus proving that the path flow pattern  $f^*$  meets the conditions of mixed user equilibrium.

Necessity:

Assume  $f^*$  is in the state of mixed user equilibrium. When  $f_{k,m}^w(d) > 0$ , we have  $C_{k,m}^w(d) = u_m^w(d)$ ; when  $f_{k,m}^w(d) = 0$ , we have  $C_{k,m}^w(d) \geq u_m^w(d)$ ; further, from Formula (11), we can obtain that, if  $f_{k,m}^w(d) > 0$ , then  $C_{k,m}^w(d) \leq u_m^w(d)$ . If  $f_{k,m}^w(d) > 0$  and  $f_{l,m}^w(d) > 0$ , then  $C_{k,m}^w(d) = C_{l,m}^w(d)$ , so, when  $f_{k,m}^w(d) > 0$ ,  $\rho_{kl,m}^w(d) = 0$ . When  $f_{k,m}^w(d) > 0$  and  $f_{l,m}^w(d) > 0$ , then  $\rho_{lk,m}^w(d) = 0$ ; hence,  $f_{k,m}^w(d) \sum \rho_{kl,m}^w(d) = 0$ . According to Formula (11), we obtain the following: when  $f_{k,m}^w(d) > 0$ ,  $f_{k,m}^w(d+1) = f_{k,m}^w(d)$ ; when  $f_{k,m}^w(d) = 0$ , we have  $f_{k,m}^w(d) \sum \rho_{kl,m}^w(d) = 0$ ; and, when  $f_{l,m}^w(d) > 0$ ,  $\rho_{lk,m}^w(d) = 0$  and, hence,  $\sum f_{l,m}^w(d) \rho_{lk,m}^w(d) = 0$ . Further, from Formula (11), we can infer that, if  $f_{k,m}^w(d) = 0$ , then  $f_{k,m}^w(d+1) = f_{k,m}^w(d)$ , i.e., the path flow pattern  $f^*$  belongs to the steady-state path flow pattern.  $\square$

#### 4. Model Solving Algorithm

Step 1: Proceed with initialization and input the model parameters.

Step 2 : Let  $d = 0$  and  $f_{k,m}^w(0) = 0$ ; calculate the generalized travel costs of each segment to obtain the generalized travel costs of the path.

Step 3: Proceed with the flow adjustment ratio. According to the generalized travel costs of different vehicles, calculate the proportion  $\rho_{kl,m}^w(d)$  of the  $m$ -th type of traveler from path  $k$  to path  $l$  between the OD pair  $w$  on day  $d$  using Formula (11).

Step 4: Proceed with path choice adjustment. Based on the flow adjustment ratio, calculate the traffic volume  $f_{k,m}^w(d+1)$  of the  $m$ -th type of traveler on path  $k$  between the OD pair  $w$  on day  $d+1$  using Formula (10).

Step 5 : Conduct the convergence test. For the set convergence standard  $\varepsilon$ , if  $\left| f_{k,m}^w(d+1) - f_{k,m}^w(d) \right| \leq \varepsilon$ , then stop iteration; otherwise, go to step 2 and let  $d = d + 1$ .

Flow chart of the model calculation process is shown in Figure 1.

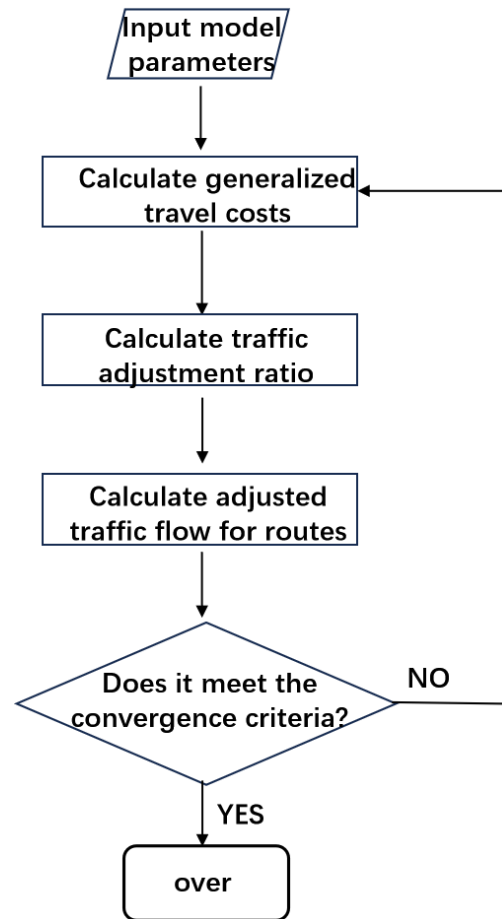


Figure 1. Flow chart of the model calculation process.

## 5. Case Analysis

### 5.1. Parameter Settings

The Nguyen–Dupuis (N-D) network is used for the case analysis, as shown in Figure 2. The N-D network consists of 13 nodes, 19 sections, 4 OD pairs, and 25 paths. The numbers on the sections in the figure represent the section numbers, while the numbers inside the circles represent the node numbers. Additional information about the network can be found in the tables below.

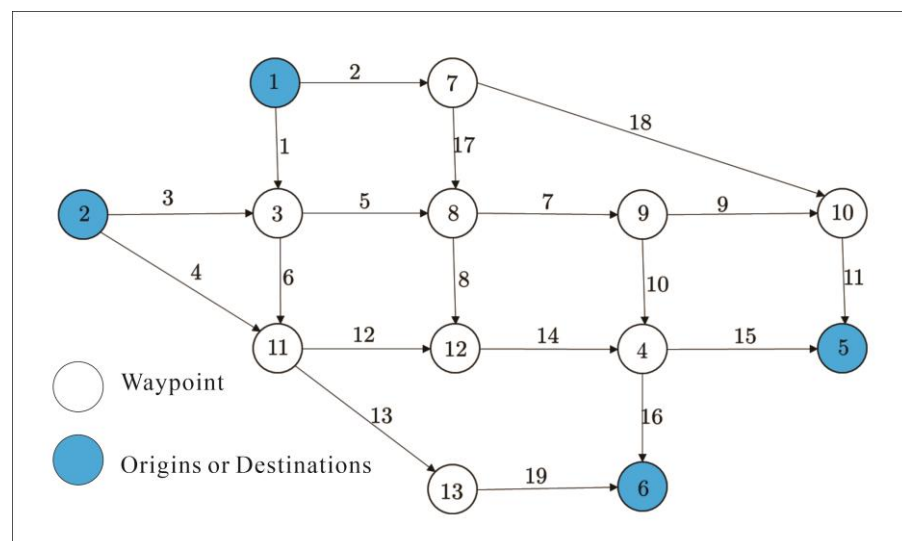


Figure 2. Example network diagram.

The traffic demand settings for the OD pairs in the N-D network are shown in Table 1.

**Table 1.** OD indicates the traffic requirement.

Origins	Destinations	
	5	6
1	1900	1500
2	1300	800

The section parameters and path information in the N-D network are shown in Tables 2 and 3.

**Table 2.** Network section parameter.

Section Number	Section Length (km)	Free Flow Time (h)	Passage Capacity (pcu/h)
1	2	0.2	800
2	2	0.2	800
3	2	0.2	800
4	4	0.3	600
5	2	0.2	800
6	2	0.2	800
7	2	0.2	800
8	2	0.2	800
9	2	0.2	800
10	2	0.2	800
11	2	0.2	800
12	2	0.2	800
13	4	0.3	600
14	2	0.2	800
15	2	0.2	800
16	2	0.2	800
17	2	0.2	800
18	6	0.4	500
19	2	0.2	800

**Table 3.** Path information table.

OD Pair	Path Number	Passing Nodes	Passing Sections
1-5	1	1-7-10-5	2-18-11
	2	1-7-8-9-10-5	2-17-7-10-15
	3	1-7-8-9-4-5	2-17-7-10-15
	4	1-7-8-12-4-5	2-17-8-14-15
	5	1-3-8-9-10-5	1-5-7-9-11
	6	1-3-8-12-4-5	1-5-8-14-15
	7	1-3-11-12-4-5	1-6-12-14-15
	8	1-3-8-9-4-5	1-5-7-10-15
1-6	1	1-7-8-9-4-6	2-17-7-10-16
	2	1-7-8-12-4-6	2-17-8-14-16
	3	1-3-8-9-4-6	1-5-7-10-16
	4	1-3-8-12-4-6	1-5-8-14-16
	5	1-3-11-12-4-6	1-6-12-14-16
	6	1-3-11-13-6	1-6-13-19

**Table 3.** Cont.

OD Pair	Path Number	Passing Nodes	Passing Sections
2-5	1	2-3-8-9-10-5	3-5-7-9-11
	2	2-3-8-9-4-5	3-5-7-10-15
	3	2-3-8-12-4-5	3-5-8-14-15
	4	2-3-11-12-4-5	3-6-12-14-15
	5	2-11-12-4-5	4-12-14-15
2-6	1	2-3-8-9-4-6	3-5-7-10-16
	2	2-3-8-12-4-6	3-5-8-14-16
	3	2-3-11-12-4-6	3-6-12-14-16
	4	2-11-12-4-6	4-12-14-16
	5	2-11-13-6	4-13-19
	6	2-3-11-13-6	3-6-13-19

In this case study, the traffic volume is considered as the peak-hour traffic volume for the day, with parameter values derived from the research of Kou Zhao [11], as shown in the Table 4.

**Table 4.** Example parameter value.

Parameter	Value	Parameter	Value
$d$	150 days	$VOT_H$	1 CNY/h
$\zeta$	0.0000001	$VOT_C$	0.5 CNY/h
$\theta_H^w$	0.05	$\theta_C^w$	0.5
$\eta_w(0)$	0.5	$\sigma_w$	0.5
$\beta_1$	0.4	$\beta_2$	0.7

5.2. Result Analysis

Using the parameter values mentioned above, we can derive the daily evolution process of mixed traffic flow on each path in the case study network, the daily evolution of generalized costs on each path, and the evolution of path flows for both CAVs and HDVs.

The daily evolution process of mixed traffic flow on each path for every OD pair is shown in Figures 3–6.

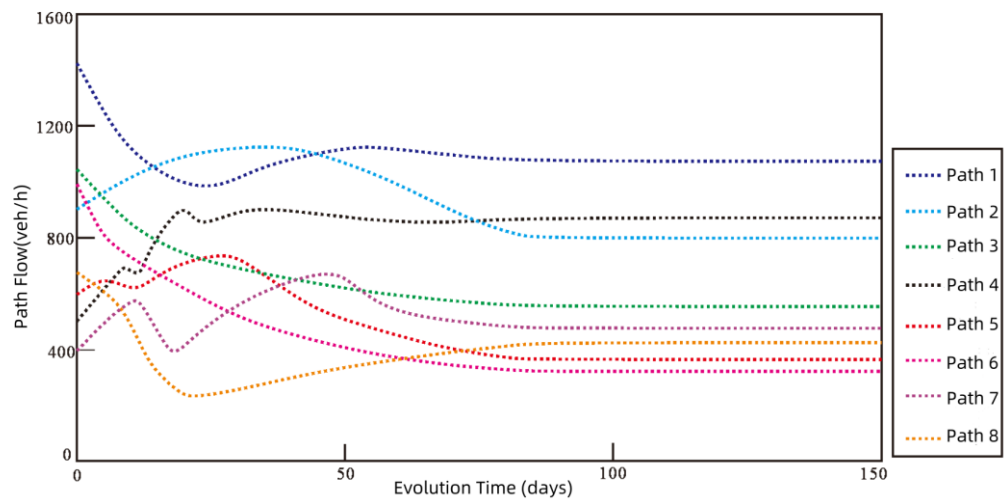


**Figure 3.** The evolution process of OD traffic to paths 1–5.

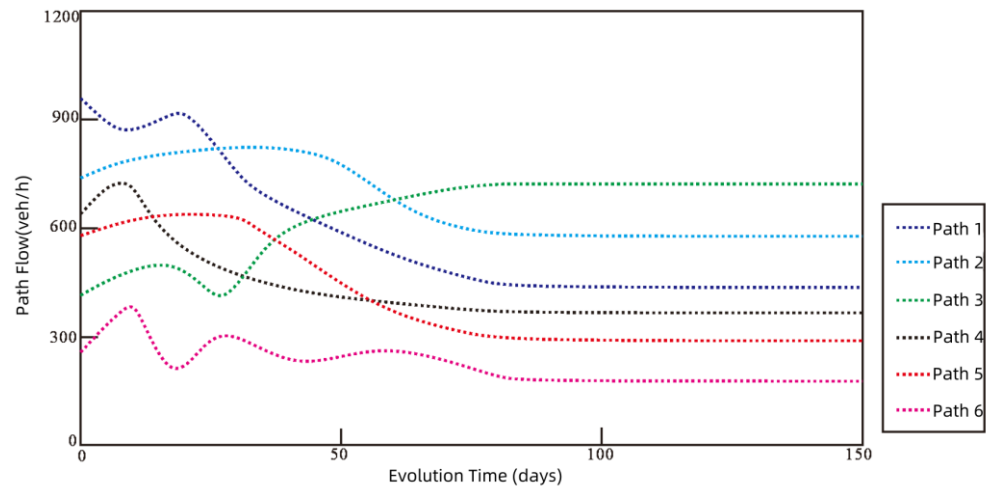


**Figure 4.** The evolution process of OD traffic to paths 1–6.

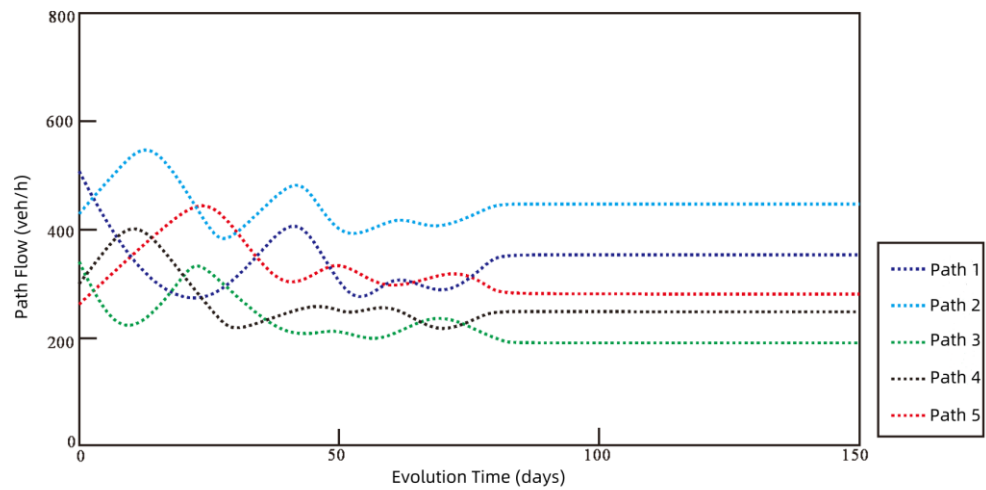


**Figure 5.** The evolution process of OD traffic to paths 2–5.

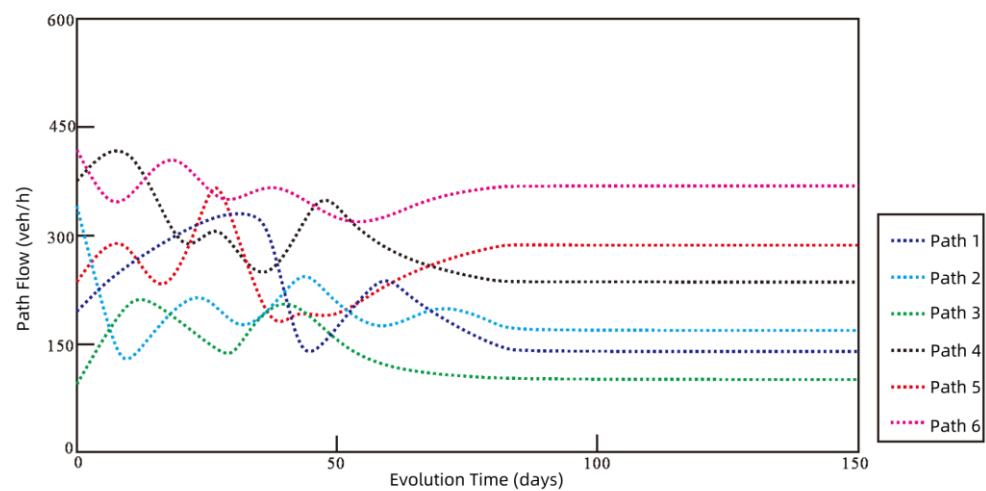


**Figure 6.** The evolution process of OD traffic to paths 2–6.

Based on the daily evolution process of mixed traffic flow on each path for every OD pair, it is evident that the path flow between each OD pair in the case network converges to the mixed-equilibrium state. The mixed flow exhibits more significant fluctuations during the first 80 days, after which it stabilizes and reaches its equilibrium state.

The evolution of generalized travel costs along each path over time for every OD pair is illustrated in Figures 7–10.

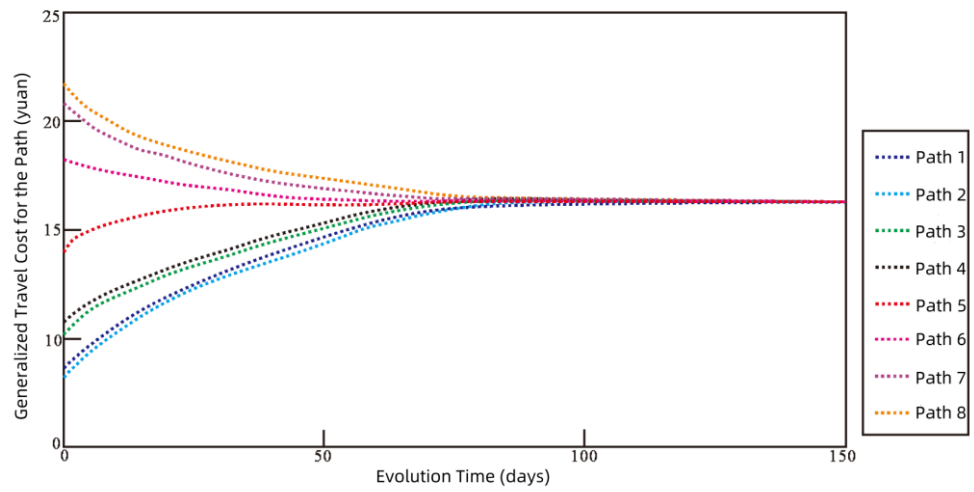


Figure 7. The evolution process of generalized travel costs for the OD pairs of paths 1–5.

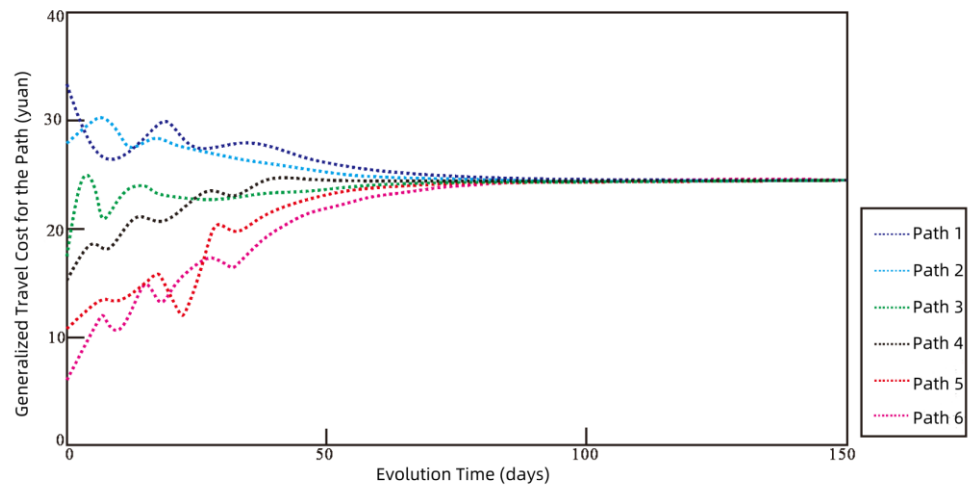


Figure 8. The evolution process of generalized travel costs for the OD pairs of paths 1–6.

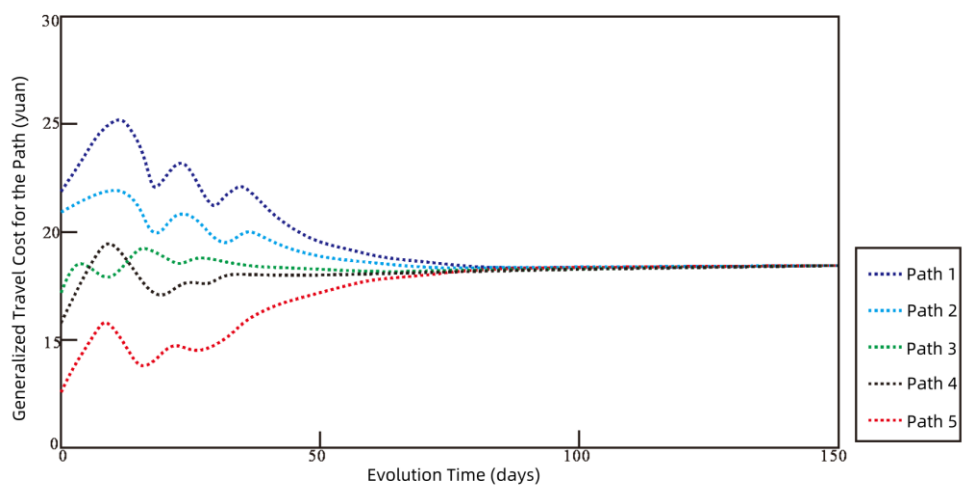
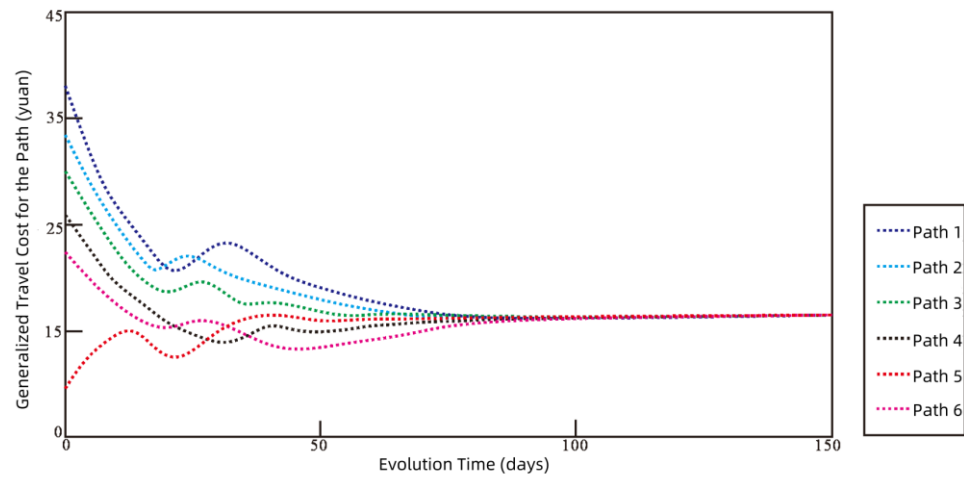


Figure 9. The evolution process of generalized travel costs for the OD pairs of paths 2–5.



**Figure 10.** The evolution process of generalized travel costs for the OD pairs of paths 2–6.

As observed in Figures 7–10, the evolution of path flows aligns with the changes in generalized travel costs. During the initial 80 days, the generalized travel costs exhibit significant fluctuations. Beyond this period, these costs for each path gradually stabilize and converge to a consistent value. This indicates that, as the mixed flow evolves, the entire traffic system achieves a state of mixed equilibrium. Similarly to real-world scenarios, in the initial stages of implementing traffic management policies, drivers' acquisition and understanding of the policies, as well as their subsequent decisions, will all contribute to fluctuations in generalized travel costs. After a period of time (approximately 80 days), the majority of drivers on the road have fully grasped the policies and have solidified their decisions based on their individual needs. Consequently, the generalized travel costs gradually stabilize and converge.

Next, the evolution process of CAV and HDV path flows is analyzed using OD pair 1–5 as an example. Figures 11 and 12 illustrate the evolution of path flows for CAVs and HDVs, respectively.

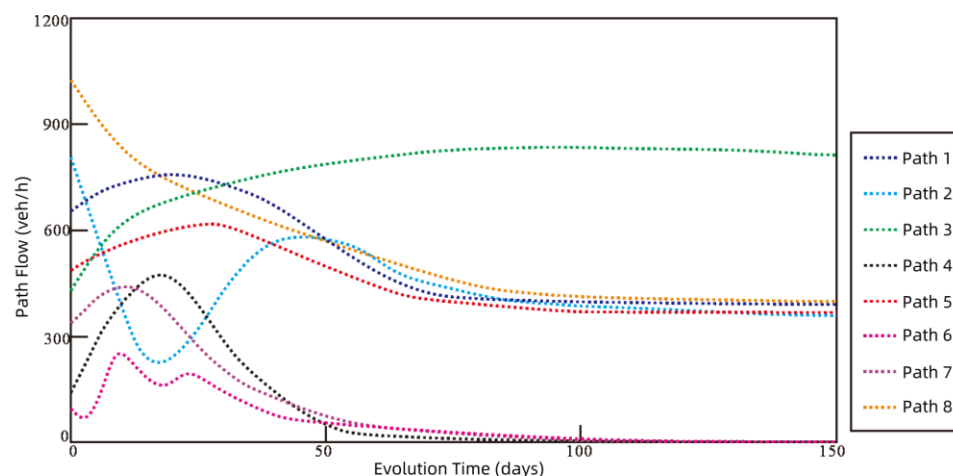


**Figure 11.** The evolution process of HDV traffic on OD paths 1–5.

Figures 11 and 12 demonstrate that the CAV flow experiences significant fluctuations during the early stages, reaching a near-equilibrium state within 60 days. In contrast, the HDV flow fluctuates less initially but requires a longer period to stabilize, achieving near-equilibrium after 80 days. Using path 2 of OD pair 1–5 as an example, the HDV flow decreases significantly during the first 40 days, while the CAV flow increases considerably. Notably, the mixed flow shows minimal fluctuation during this period due to the joint

evolution of CAV and HDV flows. Approaching the mixed-equilibrium state after 80 days, the mixed flow is distributed across all paths, with the HDV flow dropping to zero on paths 4, 6, and 7, and the CAV flow becoming zero on paths 1, 3, and 5. Both vehicle types, however, maintain flows on paths 2 and 8. This distribution arises from the presence of three user types and two vehicle types in the network, each following distinct path selection criteria. Furthermore, the differences in parameter values within the case network influence the generalized travel costs across paths. These variations, coupled with the differing sensitivities of vehicle types to impedance changes, result in varying stabilization times for path flows and generalized travel costs across OD pairs.

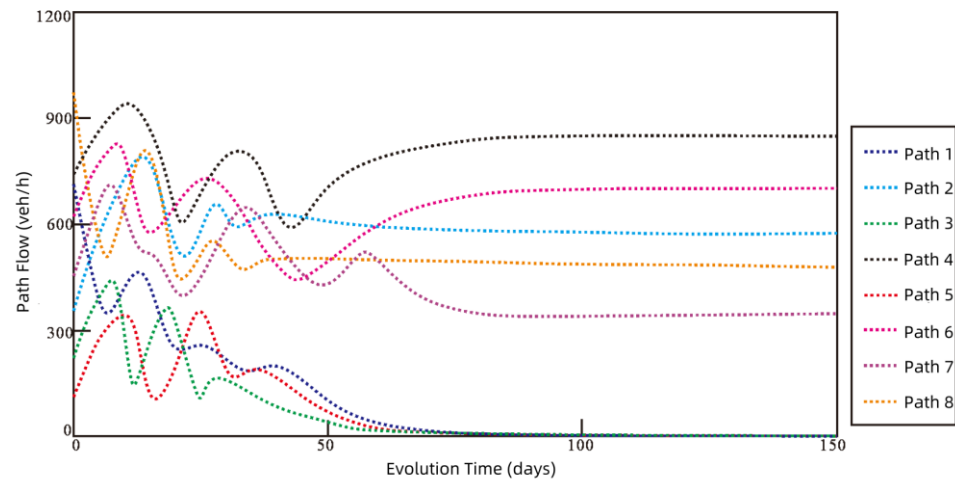


**Figure 12.** The evolution process of CAV traffic on OD paths 1–5.

### 5.3. Sensitivity Analysis

Next, we examine the impact of CAV sensitivity,  $\theta_m^w$ , on the evolution process of mixed flow. By keeping other parameters constant, the sensitivity  $\theta_C^w$  of CAV is set to 0.3, 0.4, 0.5, and 0.6, respectively. The evolution process of the mixed flow for OD pair 2–5 is analyzed to assess how different sensitivity levels influence the dynamics. When the sensitivity of CAV is 0.5, the evolution process is illustrated in Figure 5. Additionally, the evolution processes corresponding to other sensitivity levels are depicted in Figures 13–15.

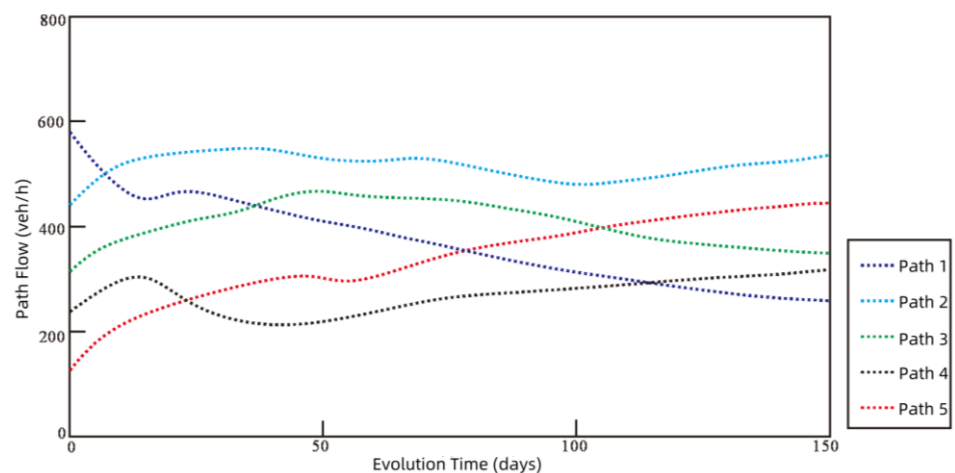


**Figure 13.** Process of path traffic evolution in  $\theta_C^w = 0.3$ .

As can be seen from Figures 12–14, when  $\theta_C^w$  is 0.3, the evolution of path flow is relatively smooth, and the network does not reach a mixed-equilibrium state after 150 days; when  $\theta_C^w$  is 0.4, the mixed flow fluctuates more obviously in the first 40 days, and the

network reaches a mixed-equilibrium state after 100 days. As can be seen from Figure 6, when  $\theta_C^w$  is 0.5, the path flow fluctuates significantly in the first 50 days, and the network reaches a mixed-equilibrium state after 80 days; when  $\theta_C^w$  is 0.6, the path flow fluctuates even more strongly in the first 30 days, and the network reaches a mixed-equilibrium state after 60 days. From this, it can be found that different traveler response sensitivities  $\theta_C^w$  of CAV can change the evolution process of mixed flow. That is, as the response sensitivity of CAV to impedance changes increases, the fluctuation of mixed traffic volume in the early stage of evolution increases, and the time required for the network to reach a mixed-equilibrium state decreases.

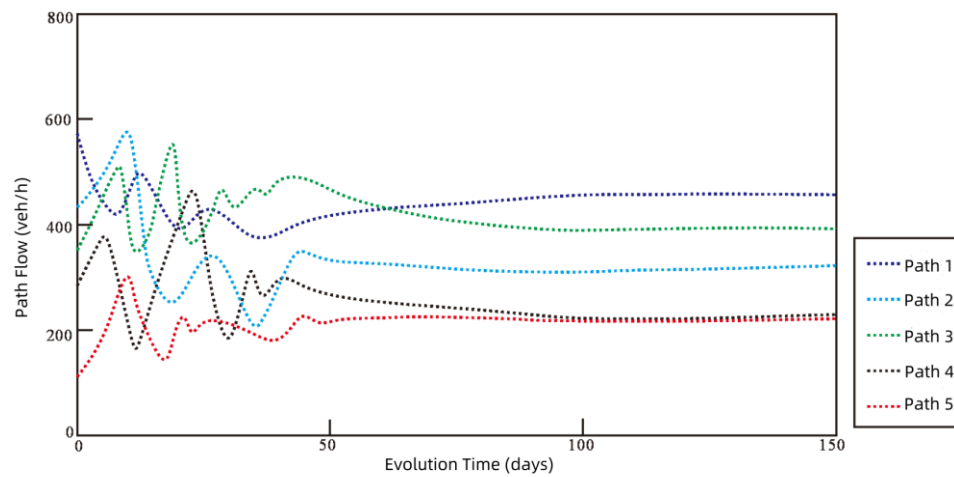


**Figure 14.** Process of path traffic evolution in  $\theta_C^w = 0.4$ .

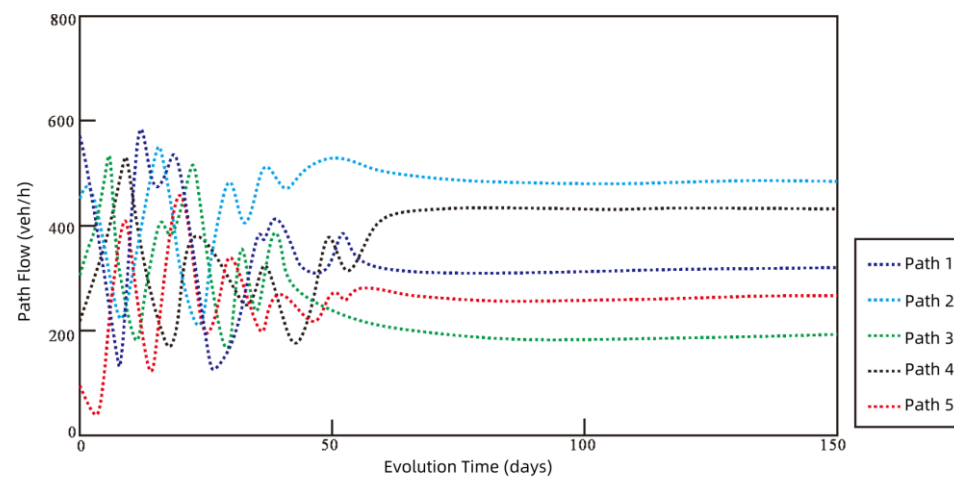


**Figure 15.** Process of path traffic evolution in  $\theta_C^w = 0.6$ .

## 6. Chapter Summary

Firstly, based on the travel characteristics of CAVs and HDVs, user groups in the connected autonomous driving environment are categorized into three types. The first type consists of users who fully comply with CAV operations and follow the system optimal (SO) criterion. The second type includes users who do not fully comply with CAV operations and follow the user equilibrium (UE) criterion. The third type comprises HDV drivers who adhere to the stochastic user equilibrium (SUE) criterion. A method for calculating travel costs for CAVs and HDVs is developed, incorporating both travel time and energy consumption costs. The proportional-switch adjustment process (PAP) is employed to establish a daily evolution model of mixed traffic flow in the connected autonomous driving environment, and the fundamental properties of this model are formally proven.

Finally, numerical simulations are performed on the N-D network to validate the rationality and effectiveness of the proposed daily evolution model of mixed traffic flow, and a sensitivity analysis is conducted to examine the impact of vehicles' response sensitivity within the model.

**Author Contributions:** Writing—original draft preparation, Y.H.; writing—review and editing, Y.H. and H.Z.; and supervision, A.K. All authors have read and agreed to the published version of the manuscript.

**Funding:** This research was funded by the Scientific Research Project of the Hunan Provincial Department of Education (nos. 20A023 and 20A009).

**Data Availability Statement:** The original contributions presented in this study are included in the article. Further inquiries can be directed to the corresponding author.

**Conflicts of Interest:** The authors declare no conflicts of interest.

## References

1. China Society of Automotive Engineers, National Intelligent and Connected Vehicle Research Institute. *Report on the Development of China's Intelligent and Connected Vehicle Industry (2019)*; Social Sciences Academic Press: Beijing, China, 2019; pp. 20–21.
2. Levin, M.W.; Boyles, S.D. Effects of Autonomous Vehicle Ownership on Trip, Mode, and Route Choice. *Transp. Res. Rec.* **2015**, *2493*, 29–38. [[CrossRef](#)]
3. Chen, Z.B.; He, F.; Zhang, L.H.; Yin, Y.F. Optimal deployment of autonomous vehicle lanes with endogenous market penetration. *Transp. Res. C-Emer.* **2016**, *72*, 143–156. [[CrossRef](#)]
4. Li, R.J.; Liu, X.B.; Nie, Y. Managing partially automated network traffic flow: Efficiency vs. stability. *Transp. Res. B-Meth* **2018**, *114*, 300–324. [[CrossRef](#)]
5. Zhang, K.N.; Nie, Y. Mitigating the impact of selfish routing: An optimal-ratio control scheme (ORCS) inspired by autonomous driving. *Transp. Res. C-Emer.* **2018**, *87*, 75–90. [[CrossRef](#)]
6. Wang, J.; Peeta, S.; Lu, L.L.; Li, T. Multiclass information flow propagation control under vehicle-to-vehicle communication environments. *Transp. Res. B-Meth* **2019**, *129*, 96–121. [[CrossRef](#)]
7. Cantarella, G.E.; Velonà, P.; Watling, D.P. Day-to-day Dynamics & Equilibrium Stability in A Two-Mode Transport System with Responsive bus Operator Strategies. *Netw. Spat. Econ.* **2015**, *15*, 485–506.
8. Li, X.W.; Yang, H. Dynamics of modal choice of heterogeneous vehicles with responsive transit services. *Transp. Res. C-Emer.* **2016**, *68*, 333–349. [[CrossRef](#)]
9. Liu, W.; Li, X.W.; Zhan, F.N.; Yang, H. Interactive travel choices and traffic forecast in a doubly dynamical system with user inertia and information provision. *Transp. Res. C-Emer.* **2017**, *85*, 711–731. [[CrossRef](#)]
10. Liang, Y. Research on Multi-Time Scale Traffic Congestion Toll Model Considering Efficiency and Environment. Master's Thesis, Beijing Jiaotong University, Beijing, China, 2019.
11. Zhao, K. Research on the Day-to-Day Evolution Model and Weekly Intervention Strategies for Dual-Mode Transportation. Master's Thesis, Beijing Jiaotong University, Beijing, China, 2021.
12. Yi, Y. Research on the Dynamic Evolution of Network Traffic Flow in a Mixed Human-Machine Driving Environment. Master's Thesis, Changsha University of Science and Technology, Changsha, China, 2022.
13. Xu, K. Research on the Day-to-Day Dynamic Evolution of Traffic Flow Based on Prospect Theory. Master's Thesis, South China University of Technology, Guangzhou, China, 2019.
14. Calvert, S.C.; Van Den Broek, T.A.; van Noort, M. In Modelling cooperative driving in congestion shockwaves on a freeway network. In Proceedings of the 2011 14th International IEEE Conference on Intelligent Transportation Systems (ITSC), Washington, DC, USA, 5–7 October 2011; pp. 614–619.
15. Wadud, Z. Fully automated vehicles: A cost of ownership analysis to inform early adoption. *Transp. Res. A-Pol.* **2017**, *101*, 163–176. [[CrossRef](#)]
16. Zhang, S.J.; Wu, Y.; Liu, H.; Huang, R.K.; Un, P.K.; Zhou, Y.; Fu, L.X.; Hao, J.M. Real-world fuel consumption and CO (carbon dioxide) emissions by driving conditions for light-duty passenger vehicles in China. *Energy* **2014**, *69*, 247–257. [[CrossRef](#)]

**Disclaimer/Publisher's Note:** The statements, opinions and data contained in all publications are solely those of the individual author(s) and contributor(s) and not of MDPI and/or the editor(s). MDPI and/or the editor(s) disclaim responsibility for any injury to people or property resulting from any ideas, methods, instructions or products referred to in the content.